Article

Photoluminescent Transparent Wood with Excellent UV-Shielding Function

Rui Xu, Jian Gan, Jing Wang, Weiying Zhao, Ke Tong, and Yan Wu*
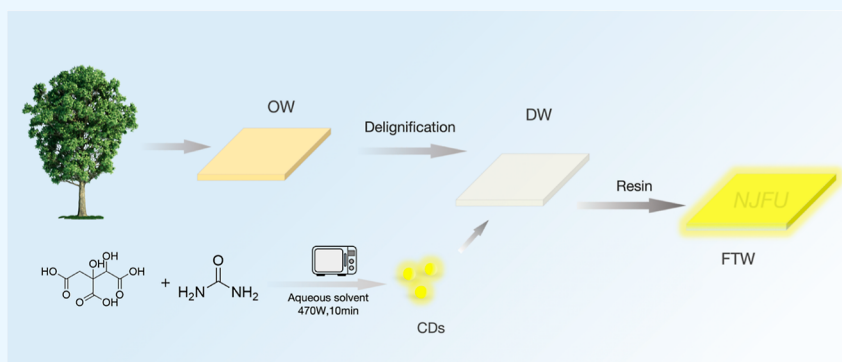
Read Online

ACCESS | Metrics & More | Article Recommendations | Supporting Information

ABSTRACT: At present, light transmission, energy saving, environmental protection, and UV-shielding materials are very important for optimizing indoor living environment. Here, a fluorescent transparent wood (FTW) with UV-shielding function was prepared by encapsulating a carbon quantum dot and epoxy resin into a delignification wood template. FTW exhibits excellent optical transmittance (about 91%), water absorption stability (weight gain rate less than 9%), longitudinal tensile strength (139 MPa), and UV-shielding properties. Due to the photoluminescence characteristics of the carbon quantum dot and the natural cellulose skeleton of wood, FTW can show uniform luminescence under ultraviolet lamps. At the same time, it has remarkable UV-shielding performance. This kind of photoluminescent transparent wood with a UV-shielding function also has the potential to be applied to fields such as electromagnetic shielding and harmful gas detection.

1. INTRODUCTION

Due to the destruction of the ozone layer and the increasing intensity of ultraviolet radiation on the ground, it inevitably causes certain damage to the human immune system and skin, which not only accelerates the aging of indoor materials.[1] The development of light-transmitting materials with UV-shielding function to alleviate the aging of indoor household items is a long-term goal of scientific researchers.[2] General light-transmitting materials, such as architectural glass, have the disadvantages of slow degradation, poor mechanical properties, and poor UV-shielding effect.[3]

In recent years, transparent wood has been widely recognized and applied in various light-transmitting materials because of its light transmittance and excellent mechanical properties.[4] It has many excellent properties such as light-weight, low thermal conductivity, adjustable light transmittance, and haze degree. Transparent wood instead of glass is not only safe and difficult to break, but also has a certain privacy effect because of its high haze.[5−8] The preparation principle of transparent wood is mainly to remove the lignin in the wood or the color substances in the lignin and impregnate the wood with a resin with a similar refractive index to achieve the effect of light transmission.

Li et al.[9] developed TW composites that have excellent insulation and optical properties and can be used as potential substitutes for glass. In addition, some researchers have also studied functional applications of transparent wood, such as luminous properties,[10,11] electromagnetic shielding,[12,13] temperature sensors,[14] and so on. Yu et al.[15] obtained a transparent wood with near-infrared shielding capability and high visible light transparency by dispersing $CsWO_3$ nanoparticles in a prepolymerized methyl methacrylate solution and introducing them to a delignification template. Wang et al.[16] developed a transparent device with electromagnetic shielding, using the assembly of a transparent bamboo and ITO film. The main components of the wood template after lignin removal are cellulose and hemicellulose, but cellulose itself does not have the ability to absorb UV light. Therefore, it is of great

significance to improve the UV-shielding ability of transparent wood by adding functional particles with UV absorption ability to delignify wood template. At present, metal oxide nanoparticles are added to most ultraviolet shielding materials, such as TiO_2, which has the advantages of low price, good stability, and good antiultraviolet effect. Qiu et al.[17] prepared ultraviolet-shielded transparent wood by adding a modified antimony-doped tin oxide (ATO) to it. When the ATO additive amount is 0.7 wt %, the UV-shielding effect is as high as 80%. When used as a transparent wood window, it can effectively reduce the damage of ultraviolet light to the human skin. However, the photocatalytic properties of metal oxide particle lead to mutagenesis, oxidation, and other reactions that damage the protected matrix, and increase the harm of ultraviolet light.[18] Carbon quantum dots (CDs) is a new kind of carbon nanomaterial used in photoluminescence, which has the advantages of low toxicity, hydrophilic, and ultraviolet absorption.[19−23] CDs were synthesized by microwave using citric acid as a precursor and urea as dopant. This method is convenient, fast, and cost-effective, which can be applied to batch and large-scale preparation of CDs, and is also environmental friendly.[24] Gan et al.[25] prepared a composite film with light conversion capability by adding CDs to a cellulose film. It is a feasible method to use the excellent UV absorption capacity of CDs to develop energy-saving building composites with a light conversion function.

Herein, a kind of photoluminescent transparent wood with a UV-shielding function is reported. Using the function and structure of transparent wood and the ultraviolet absorption capacity of CDs,[26] the cellulose pipeline of lignified wood was used as the dispersive medium of CDs, and then filled with epoxy resin for composite preparation. Photoluminescent transparent wood [fluorescent transparent wood (FTW)] exhibits high light transmittance, high haze, and the ability to absorb ultraviolet rays. In addition, FTW has excellent mechanical properties (tensile rise, impact resistance, and bending resistance) and thermal stability as well as water resistance. FTW has great potential as green and safe UV-shielding materials.

2. EXPERIMENTAL SECTION

2.1. Materials and Equipment.
Canadian white maple (OW) was provided by Deqing Meilun Decorative Materials Co., Ltd. The air-dry density of maple was 0.467 g/cm³, the absolute dry density was 0.53 g/cm³, and the moisture content was 11.7%. The specification used was 50 mm × 50 mm × 0.5 mm (length × width × thickness). Sodium chlorite, concentration 80%, supplied by Shanghai McLean Co., Ltd. Glacial acetic acid, analytical grade, provided by China Nanjing Chemical Reagent Co., Ltd. Anhydrous ethanol, analytically pure, provided by China Nanjing Chemical Reagents Co., Ltd. H758 epoxy resin and H758 epoxy resin curing agent were purchased from Qingdao Viscotuli Co., Ltd. Citric acid was provided by Sinopharm Group Chemical Reagent Co., Ltd. Urea was provided by Sinopharm Group Chemical Reagent Co., Ltd. Ultrapure water was laboratory made. Dialysis bag, 100DA, was supplied by Yibo Bio Ltd.

The instruments used during the preparation process include electric heating constant temperature blast drying oven, model: DHG-9643BS-III, provided by Shanghai Xinmiao Medical Equipment Manufacturing Co., Ltd.; electronic balance, model: UTP-313, provided by Shanghai Huachao Electric Appliance Co., Ltd. SCIENCETOOL Laboratory oil-free vacuum pump, model: R410, provided by US Suntex International Group; plastic vacuum dryer, model: PC-3, provided by Shanghai Sanmusk Industrial Co., Ltd. Constant temperature water tank for digital display 3, model: HH-600, provided by Jintan Guowang Experimental Instrument Factory; microwave oven, output power 700 W, model: P70F20CL-DG(B0), provided by Guangdong Galanz Microwave Household Appliances Manufacturing Co., Ltd. Collector type constant temperature heating magnetic stirrer, model: DF-101Z, was obtained by Nanjing Wozhong Instrument Equipment Co., Ltd. Freeze-dryer, model: FD-1A-50, provided by Shanghai Birang Instrument Manufacturing Co., Ltd.

2.2. Experimental Methods.
In this experiment, acidic sodium chlorite solution was used to prepare a delignified wood template (DW). Citric acid and urea were used to prepare CDs. Then the DW sample was soaked in the prepared carbon quantum dot ethanol solution so that the carbon quantum dot was distributed into the cellulose skeleton of the wood. Finally, epoxy resin was used for filling and curing.

2.2.1. Pre-processing. The OW samples were dried in a constant temperature oven at 102 °C for 12 h. The absolutely dried OW samples were set out for the next experiment.

2.2.2. Preparation of the Delignified Wood Templates. A sodium chlorite aqueous solution with a concentration of 3.7 wt % was prepared. Then drop appropriate amount of glacial acetic acid was dropped into the solution, so that the pH value of the solution was adjusted to 4.6. The samples were placed in the solution and heated by immersion in a digital triple-use thermostat for 2 h. Then, the samples were placed in ultrapure water and allowed to stand for 20 min in a water bath at 80 °C. Repeat the operation three times to wash away the residual chemical reagents in the delignified wood templates. Finally, the samples were placed in anhydrous ethanol solution to replace the water in the internal pores of the sample, so as to improve the permeability of the sample and obtain DW samples.

2.2.3. Preparation of CDs. First, 1 g of citric acid and 1 g of urea were dissolved in 10 mL of ultrapure water and were well stirred. Then, the mouth of the beaker was covered with plastic wrap and the mixture was put into the microwave oven for 490 W to react for 10 min. Poured 50 mL ultrapure water was poured into the cooled solution and stirred evenly to obtain carbon quantum dot solution. The carbon quantum dot solution was transferred to a centrifuge to remove the residual solid impurities. The centrifuge speed was set to 10,000 rpm, and the centrifuge time was set to 10 min. The supernatant from the centrifuge tube was transferred to a dialysis strip with a molecular interception of 100DA and dialysis was performed in flowing ultrapure water for 32 h. The solution purified by dialysis was dried by freeze-vacuum, and yellow light emitting carbon quantum dot solid powder was obtained.

2.2.4. Preparation of FTW. Carbon quantum dot ethanol solution with a concentration of 0.1‰ was prepared. The prepared DW was removed from anhydrous ethanol solution and put into a CD ethanol solution. After soaking for 48 h, the DW with photoluminescence performance was obtained. According to the weight ratio of epoxy resin to curing agent 3:1, epoxy resin impregnation solution was prepared, stirred evenly with a magnetic stirrer, and set aside. Pour an appropriate amount of epoxy resin impregnation solution into the lignified wood template and soak in a vacuum environment for 3 h. Finally, the impregnated sample was removed and put into two pieces of silica gel to ensure that the
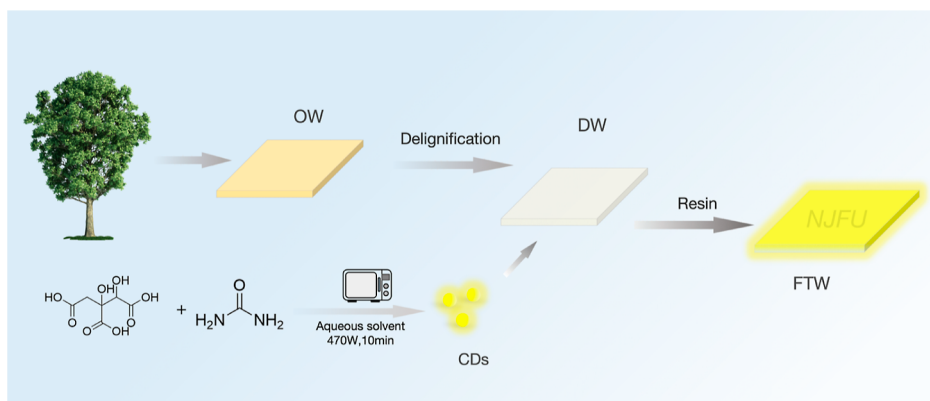
Figure 1. Graphical illustration of the design concept and construction process of FTW.
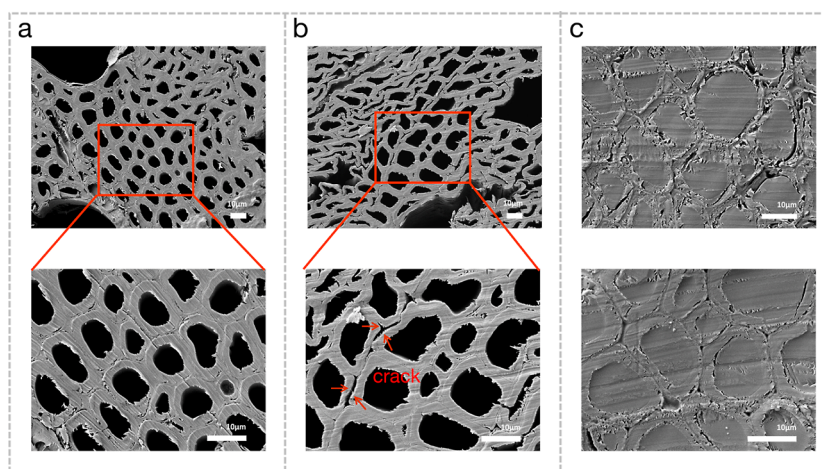
Figure 2. SEM images of the samples after delignification and transparency treatment: (a) OW; (b) DW; (c) FTW.

sample surface was smooth and then cured at room temperature for 24 h to obtain FTW (Figure 1).

3. CHARACTERIZATION

In order to facilitate the characterization of samples, the types of samples that may appear in the test are numbered in this experiment. Specifically, OW represents the original wood. DW represents wood templates after lignin removal. TW represents samples impregnated with epoxy resin. FTW represents the transparent wood which added carbon quantum dots. H758 represents epoxy resin with model number 758. Y-CDs stand for yellow fluorescent carbon quantum dots.

3.1. Field Emission Electron Microscope. The sample was cut along the transverse direction and the surface of the cut sample was polished by ultrathin slicer and then adhered to the observation disk for vacuum gold plating. JSM-7600F field emission scanning electron microscope was used to observe the cross-section and the internal morphology of the samples.

3.2. Fourier Transform Infrared Spectrum. The chemical groups of all samples were measured by Fourier transform infrared spectroscopy (FTIR, ERTEX80 V, Germany). The changes of chemical groups before and after sample processing were analyzed by observing the vibration of chemical groups under the light irradiation of $400-4000$ cm^{-1}, with a resolution of 4 cm^{-1}. The crystal structures of OW and DW were characterized and analyzed by a combined multifunctional horizontal X-ray diffractometer (XRD). The

test range is 2θ equal to $5-80°$, and the interval is equal to 0.02.

3.3. Determination of Cellulose, Hemicellulose, and Lignin Content. The relative contents of lignin, cellulose, and hemicellulose in OW and DW samples were measured according to the method of the National Renewable Energy Laboratory (NREL).

3.4. CDs Performance Test. X-ray photoelectron spectroscopy (XPS) spectra were obtained using an Ultima IV spectrometer (AXIS UltraDLD, Shimadzu, UK). The optimal excitation wavelength and emission wavelength of CDs were measured by an LS 55 fluorescence spectrophotometer. The UV absorption spectra of CDs were analyzed by a U-3900 ultraviolet/visible/near-infrared spectrophotometer.

3.5. UV Transmittance Measurements. The UV transmittance measurements of OW, DW, TW, and FTW samples were performed at $380-780$ nm using a Lambda 950 UV–visible spectrometer. Meanwhile, we measured the haze of glass and FTW at $400-800$ nm, and measured the UV absorption spectra of FTW and glass at $320-400$ nm.

3.6. Mechanical Performance Measurements. The longitudinal tensile properties of the samples were tested by an AG-IC precision electromechanical testing machine. The sample size was 20 mm $\times$ 80 mm $\times$ 0.5 mm, the standard distance was 40 mm, the tensile rate was 1 mm/min, and the maximum load force was 2500 N. The LX-D Shore rubber hardness tester was used to record the surface hardness of the sample.
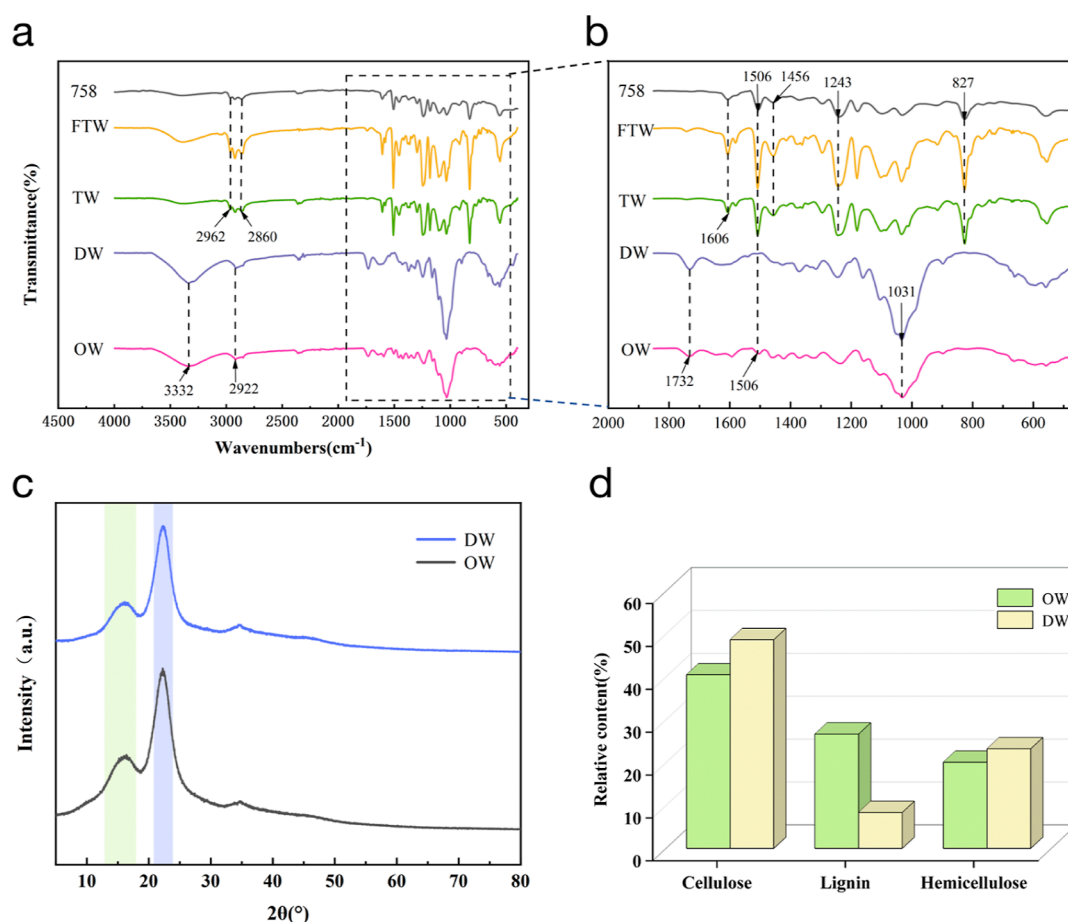
Figure 3. Sample chemical composition analysis; (a) FTIR curves of samples before and after delignification and transparency; (b) an enlarged view of the dotted box in (a); (c) XRD curves of samples before and after delignification; (d) changes in the relative contents of cellulose, lignin, and hemicellulose in wood before and after delignification.

3.7. Stability Performance Test. Thermal degradation of samples was measured using the thermogravity method and synchronous thermal analyzer (TGA, Toledo TGA/DSC1, Sweden), from 30 to 800 °C at a rate of 10 °C min⁻¹ in a nitrogen atmosphere. The weight gain rate of the sample was calculated by placing the samples in distilled water at room temperature (27 °C) for 25 h, and the mass before and after water absorption was recorded.

4. RESULTS AND DISCUSSION

4.1. Structure and Morphology Analysis of FTW. As shown in Figure 2a, the internal cell structure of the untreated wood OW is complete, the cell cavity is not collapsed, and there is almost no space between cells. After the delignification treatment, the cell walls of the wood are deformed and cracks appear between the cells (Figure 2b). Moreover, the cellular structure inside the wood was damaged to a certain extent. It indicates that the lignin is removed, and it also means that more active hydroxyl groups are exposed in the wood cellulose skeleton, which will facilitate the distribution of carbon quantum dot in the three-dimensional porous structure.

We used epoxy resin to fill the cellulose skeleton of the wood. FTW was prepared by epoxy resin which has excellent mechanical properties. From the microtopography of FTW (Figure 2c), it can be observed that the resin is fully filled into the internal pores of DW. After impregnation, the interface

between epoxy resin and wood cell wall was good, and there was basically no crack.

4.2. Chemical Composition Analysis of FTW. FTIR spectroscopy can characterize changes in the internal chemical structure of a sample by analyzing its chemical composition. From Figure 3a,b, it can be seen that the characteristic absorption peaks of OW are at 3332 cm⁻¹ (−OH tensile vibration), 2922 cm⁻¹ (C−H tensile vibration peak), 1594 cm⁻¹ (C═O group tensile vibration), and the peak at 3332 cm⁻¹ (−OH tensile vibration peak). The characteristic peaks at 1732 cm⁻¹ (stretch vibration peak of acetyl group in hemicellulose), 1506 cm⁻¹ (stretch vibration peak of aromatic ring skeleton in lignin), 1240 cm⁻¹ (stretch vibration peak of fatty acid group), and 1031 cm⁻¹ (vibration peak of aromatic C−H plane deformation assigned to lignin) are consistent with the results of previously reported literature.[27−29] These characteristic peaks correspond to the cellulose, hemicellulose, and lignin of the wood.

As shown in Figure 3b, the tensile vibration absorption peak of lignin aromatic skeleton groups disappeared at 1506 cm⁻¹ in the delignified samples, which means that the lignin was largely removed after the delignification treatment. The wave numbers of the epoxy resin H758 are 2962 cm⁻¹ (symmetric stretching vibration of C−H group on CH₃), 2860 cm⁻¹ (antisymmetric stretching vibration of C−H group on CH₃), 1606 and 1506 cm⁻¹ (asymmetric vibration band of benzene ring skeleton), 1456 and 734 cm⁻¹. The characteristic peaks at CH₃ shear
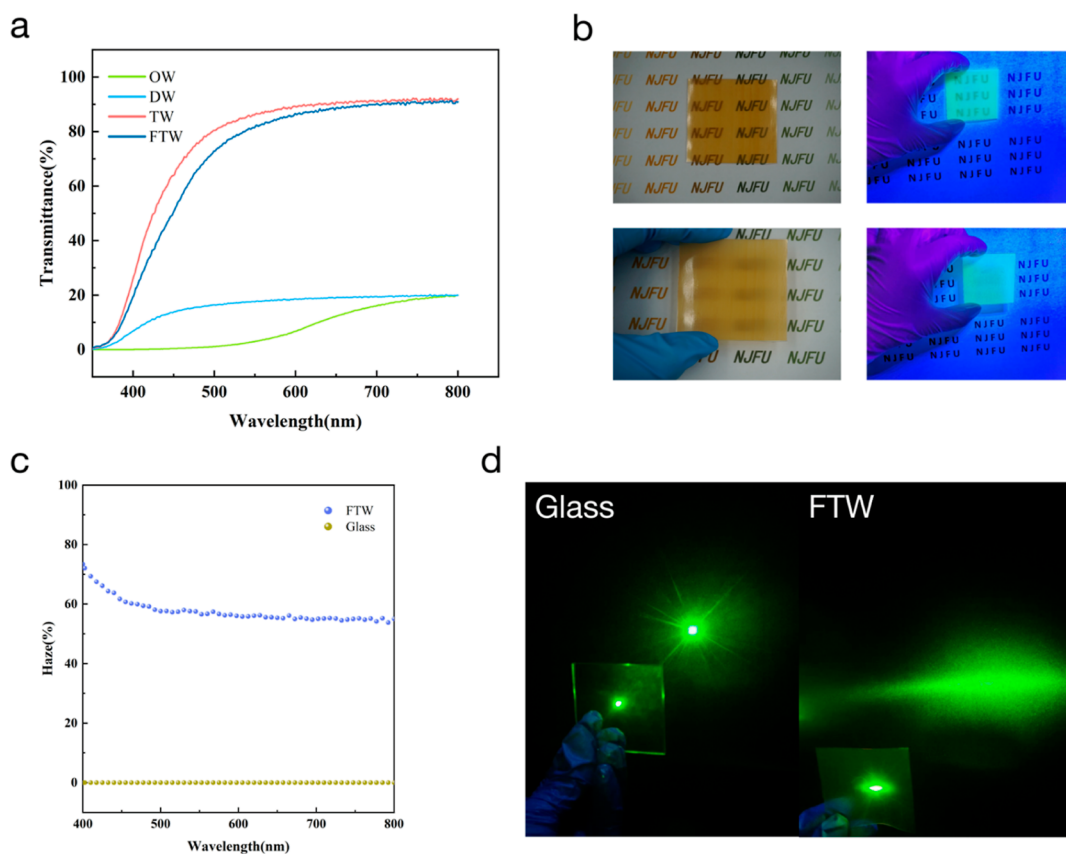
Figure 4. Transparency and haze display of FTW; (a) transmittance curves of OW, DW, TW, and FTW; (b) schematic diagram of the transmittance and haze performance of FTW under sunlight and 395 nm UV lamp irradiation; (c) haze curves of FTW and glass; (d) comparison of light scattering ability between FTW and glass.

oscillation, 1243 cm^{-1} (stretching vibration of adipose ether C−O−C) and 827 cm^{-1} (out-of-plane deformation of para-substituted benzene ring =CH) are consistent with previous studies.[30]

After vacuum impregnation resin treatment, FTW not only has the characteristic absorption peak of delignified wood but also has the characteristic peak of H758. It indicated that the transparent wood contained the molecular of delignification wood template and the molecular groups in H758, meaning that the H758 resin successfully penetrated into the delignification template.

Figure 3c shows that OW produces two major diffraction peaks at $2\theta = 16°$ and $2\theta = 22°$, which are characteristic peaks for cellulose. After the delignification treatment, the lignin relative content in the wood decreased, and the crystallinity of cellulose molecules in the inner noncrystalline zone began to increase. Therefore, the cellulose characteristic peak of the DW is stronger. Combined with FTIR tests, the cellulose molecular structure and crystal structure of the DW wood template were not damaged.

4.3. Determination of Cellulose, Hemicellulose, and Lignin Content. The relative content changes of lignin, cellulose, and hemicellulose in wood before and after delignification were studied according to the National Renewable Energy Laboratory (NREL) method. As shown in Figure 3d, the relative content of lignin in wood decreased from 26.69 to 8.40% after 2 h of treatment in acidic sodium chlorite solution. The decreased rate of the lignin relative content was 68.53%. It shows that the oxidation properties of

sodium chlorite can remove lignin of wood. The reduced lignin content represents the disappearance of "binder" which connects cellulose and hemicellulose. Hence, more pores between the cells can be used to fill the resin. The significant decrease in the relative content of lignin led to an increase in the relative cellulose content of wood, from 40.52 to 48.70%, but there was no significant change in the relative content of hemicellulose.

4.4. Ultraviolet Transmission Analysis. As shown in Figure 4b, the FTW presents high light transmittance and haze. Moreover, the FTW can still maintain this ability under UV lamp irradiation. We determined the total transmittance of OW, DW, and FTW in the visible light range from 380 to 800 nm (Figure 4a). The transmittance of OW and DW was less than 20% in the visible light range, and the transmittance of FTW was higher and higher with the increase in wavelength, reaching a maximum of 90.9%. The above test results show that the light transmittance of wood will not be greatly improved after the delignin treatment of wood, and the step that can greatly improve the light transmittance is the transparency treatment. This is because the refractive index of the resin filled in the DW coincides with the cellulose skeleton of the DW. In addition, it is worth noting that TW and FTW transmittance data differ little. This indicates that the addition of carbon dots to the wood tubing prior to resin impregnation had a minimal effect on the transmittance of the sample.

The haze of FTW is further tested, and it is found that the haze of FTW reaches more than 70%. The high light
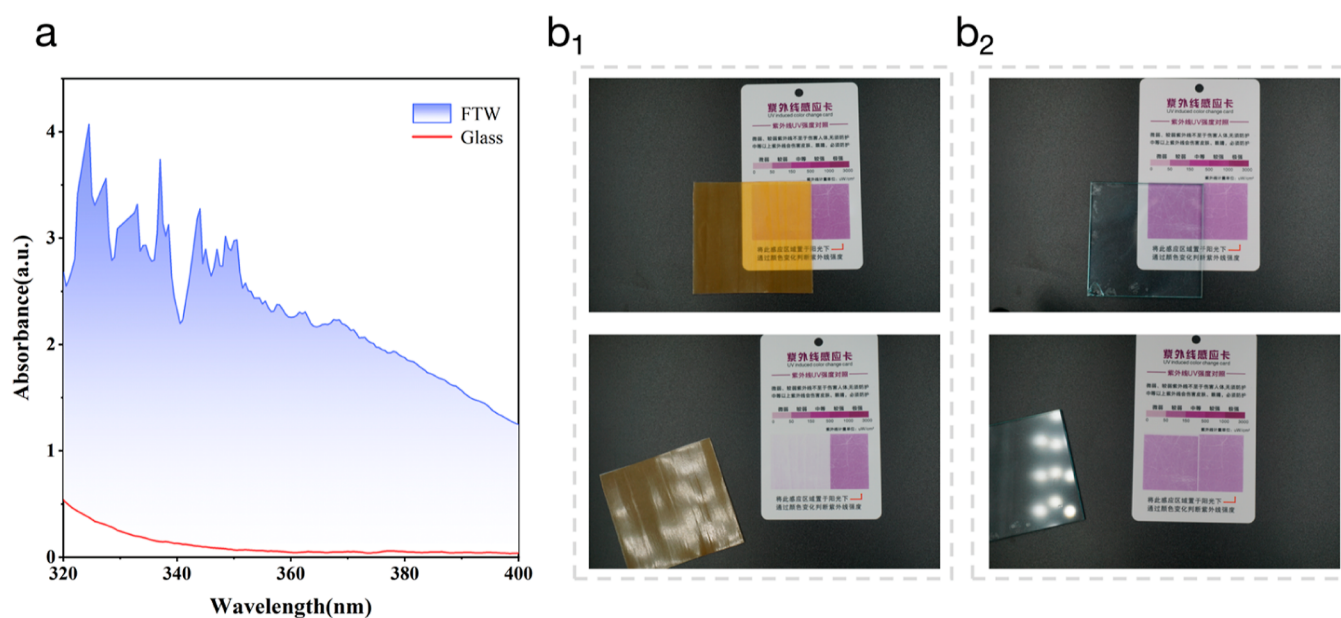
Figure 5. Schematic diagram of UV shielding of FTW; (a) comparison of UV absorption spectra between FTW and glass; (b) comparison of UV shielding ability between FTW (b1) and glass (b2).
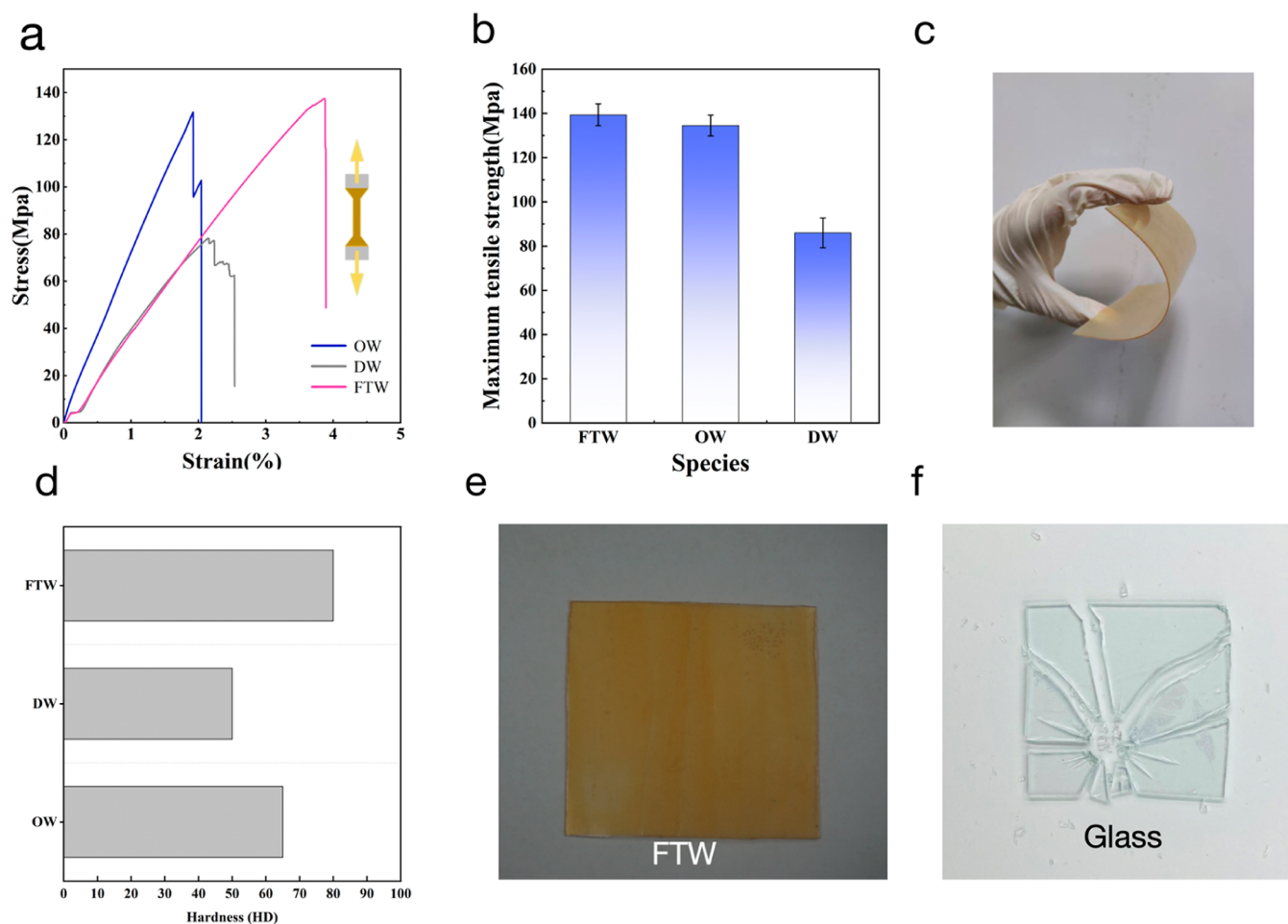
Figure 6. Illustration of mechanical property analysis of FTW. (a) Tensile stress−strain curves of OW, DW, and FTW; (b) the maximum tensile strength of OW, DW, and FTW; (c) display of bending properties of FTW; (d) surface hardness of OW, DW, and FTW; (e) the state of FTW after being struck by the metal ball; (f) the state of the glass after being struck by a metal ball; reproduced with the permission.[22] Copyright 2021, American Chemical Society.
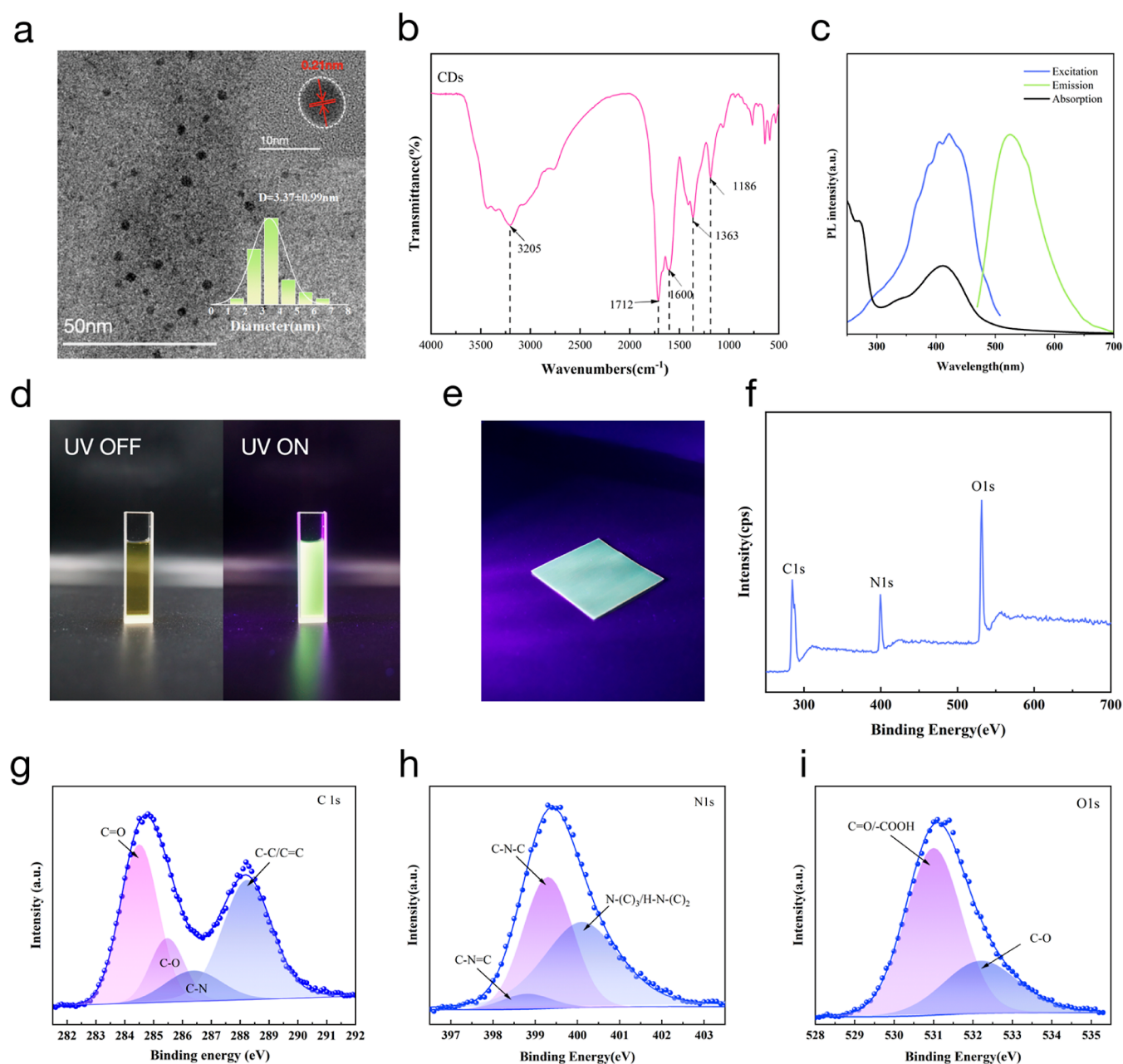
Figure 7. Structural and composition characterizations of Y-CDs. (a) High-resolution TEM images of Y-CDs. (b) FTIR spectrum of Y-CDs; (c) UV absorption spectrum and fluorescence spectrum of Y-CDs; (d) comparison of Y-CDs ethanol solution before and after ultraviolet light (395 nm) excitation; (e) the state of FTW under 395 nm UV light; (f) XPS spectrum of Y-CDs; (g) high-resolution XPS fitting results for C 1s; (h) high-resolution XPS fitting results for N 1s; (i) high-resolution XPS fitting results for O 1s.

transmissivity of FTW ensures the effective collection of light, and its high haze can expand the irradiation area of light and has a certain privacy protection effect. As shown in Figure 4d, we used the laser pointer to pass through the glass and FTW, respectively, and found that FTW can achieve more uniform and soft illumination compared with the glass material, which is meaningful for achieving a safe indoor lighting environment.

Due to the addition of carbon dots as well as the presence of residual lignin, FTW is able to absorb UV light.[31] From Figure 5a, it can be seen that FTW has obvious absorption between the UV region, while glass showed almost no UV absorption. As a proof of concept, we used UV intensity detection paper and used a 395 nm UV lamp to simulate the UV light of sunlight to demonstrate the UV-shielding performance of

FTW and glass, respectively (Figure 5b). It was found that there was almost no difference between the two sides of the color intensity detection paper in Figure 5(b2), which showed that the glass had almost no UV-shielding ability. The side covered by FTW in Figure 5(b1) is quite different from the bare side, and the side covered by FTW almost appears white, a result that further illustrates the feasibility of FTW as a light-transmitting material capable of shielding ultraviolet. Due to the unique optical properties of CDs, FTW exhibits yellow fluorescence emission while absorbing blue light. FTW's special light conversion ability can satisfy the requirements of indoor lighting, while effectively filtering sunlight ultraviolet, alleviating the aging of ultraviolet rays on the indoor
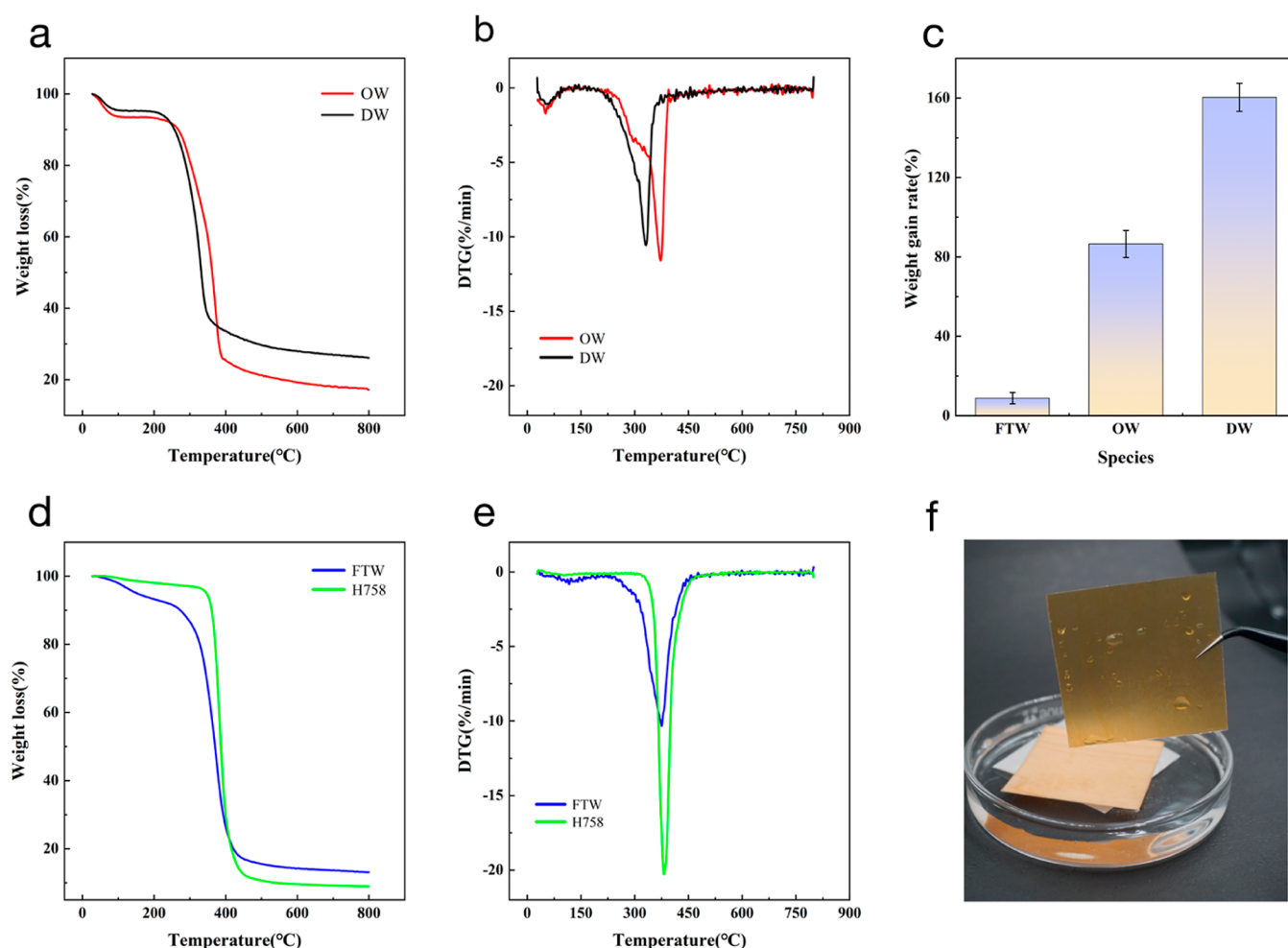
Figure 8. Schematic diagram of sample thermal stability and water stability analysis; (a) weight loss curves of OW and DW; (b) DTG curves of OW and DW; (c) the weight gain rate of OW, DW and FTW; (d) weight loss curves of FTW and H758; (e) DTG curves of FTW and H758; (f) the state of FTW after immersion in water for 25 h.

environment and providing a safer lighting environment, which is not available in glass materials.[23]

4.5. Analysis of Mechanical Properties of FTW. The reliability of the FTW was evaluated according to the mechanical tensile test. As shown in Figure 6b, it can be seen that the maximum tensile strength of DW samples decreased significantly after wood was treated in sodium chlorite solution. While DW was impregnated with resin, the maximum tensile strength of the sample was significantly increased, which reached 139 MPa. According to the microscopic morphology analysis described above, epoxy resin is fully filled into the cell cavity of wood and fully bonded with the cellulose skeleton of the cell wall. The excellent mechanical properties of epoxy resin improve the tensile properties of FTW. In addition, it is worth noting from Figure 6a that when compared with OW, the strain of FTW under the same stress increases significantly, indicating that FTW has greater elasticity. The presence of epoxy resin increases the flexibility of FTW (Figure 6c), and plays a positive role in the comprehensive mechanical strength of the material.

The hardness test (Figure 6d) showed that after delignification treatment, the surface hardness value of wood becomes lower, and after epoxy impregnation, the surface hardness value of FTW is greatly improved, surpassing that of the untreated OW sample. It is consistent with the mechanical tensile strength variation of the samples. In addition, FTW also shows superior impact resistance compared with ordinary glass. Specifically, after being subjected to a 200 g metal ball falling from a height of 30 cm, FTW can still maintain its intact shape surface without any damage (Figure 6e). While the glass completely breaks into sharp fragments (Figure 6f).[20] It shows FTW's own flexibility gives it the ability to effectively counteract sudden impact forces and elevate indoor safety.

4.6. Performance Analysis of CDs. The morphology of the prepared Y-CDs was observed by high-resolution TEM (Figure 7a). The size distribution of the prepared carbon quantum dots is almost uniform, the particle size is less than 10 nm (Figure S2). Compared with the previously reported blue emission CDs, their lager average size distribution corresponds to the red-shift of the emission, manifesting the quantum confinement effect.[23,32] The carbon dots have lattice stripes, the lattice spacing is 0.21 nm, which corresponds to the (100) crystal plane spacing of graphite;[33] CDs with highly graphitized carbon cores could exhibit highly stable PL properties.[34,35]

From the infrared spectrum (Figure 7b), it can be seen that there is a broad absorption peak near 3205 cm^{-1}, which belongs to the stretching vibration of O−H, N−H.[36] The absorption peak at 1600 cm^{-1} belongs to the C=O stretching vibration.[29] The absorption peak at 1363 cm^{-1} belongs to the

bending vibration of N−H and O−H. The absorption peaks at 1186 cm^{-1} belong to the stretching vibrations of C−N and C−O, respectively. In conclusion, the surface of Y-CDs contains hydrophilic groups such as −OH and −COOH.

The surface composition and structure of carbon quantum dots were analyzed by XPS (Figure 7f−i) to further confirm the results of infrared spectroscopy. As can be seen from the total XPS spectrum Figure 7f, there are three peaks of C 1s (284.5 eV), N 1s (399.5 eV) and O 1s (531.5 eV), and the N element peak indicates that the N element in urea has been successfully doped into the carbon quantum dot.[37,38] In addition, it can be seen from Figure 7g−i that there are abundant oxygen-containing functional groups on the surface of carbon quantum dots, such as C=O and −COOH, which proves that carbon quantum dots are hydrophilic.

From the UV absorption curve of the carbon quantum dot in Figure 7c, it can be seen that a weak wave peak appears around 270 nm, which is formed by the C=C double bond $\pi-\pi^*$ transition on the benzene ring.[39] At the same time, a weak peak appears near 340 nm, which may be formed by the n−π^* transition of C=O on the surface of the carbon quantum dot.[40] Figure 7c, show the CD UV−vis absorption, PL emission, and excitation spectra. The maximum PL emission peak for Y-CDs was 524 nm. When the excitation wavelength is about 420 nm. The sample's picture in Figure 7d shows that under natural light, the carbon quantum dot solution is a uniform yellowish transparent color. While it shows strong yellow fluorescence under 395 nm UV lamp irradiation. When quantum dots are introduced into wood pipes, due to the anisotropic characteristics of wood, the light generated by quantum dots is guided by longitudinal fibers, which can produce a relatively uniform diffuse luminescence on the surface of wood[41] (Figure 7e).

4.7. Stability Performance. To measure the thermal stability of the samples, we performed a thermogravimetric analysis of OW, DW, FTW, and H758. From Figure 8b, it shown that the OW sample went through two stages of weight loss, starting from 100 °C (evaporation of water contained in the wood) and 250 °C (degradation of lignin, cellulose, and hemicellulose).[42,43] It can be seen from Figure 8a, DW has the same weight loss curve with OW. The weight loss curve of H758 indicated that it began to experience weightlessness around 360 °C. From the weight loss curve of FTW (Figure 8d), it can be seen that FTW both possesses the degradation behavior of OW and epoxy H758. However, it can be observed that there was a significant difference between the final residual mass of FTW and H758. The mass residual rate of FTW was 13.15%, while that of H758 was only 8.95%. From the ordinate of the weight loss peak of the DTG curve (Figure 8e), we can know that the weight loss rate of FTW is smaller than that of H758 and OW samples. Thus, the enhanced stability of FTW can be seen, and this improved thermal stability can be attributed to the interaction between the delignified wood and the resin matrix.[44,45] Based on thermogravimetric analysis, FTW exhibits superior heat resistance, which lays the foundation for its application as a light transmitting material.

The stability of FTW in water was further evaluated. The samples were immersed in room temperature water for more than 25 h. Then, the mass change rate was calculated. The equation is

$$W = \frac{M_a - M_b}{M_b} \times 100\%$$

Where W represents the weight gain rate of the samples; M_a represents the weight of the sample after water is applied; M_b represents the weight of wood before it encounters water.

According to Figure 8c, it is found that the weight gain rates of different samples after water absorption varies greatly. Due to its natural wood porous structure, OW has a large change in quality after water absorption. After the delignification treatment, the influence of this porous structure on the mass change after water absorption becomes more obvious, and the weight gain rate of DW after water absorption is as high as 160.38%. However, FTW performs very well due to the transparency treatment, with a mass change rate as low as 8.86%, and its appearance remains basically unchanged compared with that of the initial state (Figure 8f). It demonstrates the reliability of FTW in humid environments and provides laboratory proof of its use as a functional light transmittance material.

5. CONCLUSIONS

In this work, we report a photoluminescence transparency with UV shielding based on wood, epoxy, and functional particle CDs. Due to the directional arrangement of cellulose skeleton inside wood, it can provide a good propagation medium for the refraction and reflection of a light path. Therefore, the photoluminescent transparent wood can achieve uniform luminescence under the excitation of a UV lamp. Compared with our commonly used light-transmitting material, glass, FTW shows stronger UV-shielding ability and higher optical haze, which can achieve uniform and soft indoor lighting and reduce the harm of ultraviolet radiation on indoor environment aging at the same time. In addition, FTW also exhibits good mechanical tensile properties and impact resistance as well as the ability to maintain good stability in humid and high temperature environments, which further supports the concept of it becoming a green energy-saving building material that echoes the carbon neutrality of transparent buildings.

■ ASSOCIATED CONTENT

ⓢ Supporting Information

The Supporting Information is available free of charge at https://pubs.acs.org/doi/10.1021/acsomega.3c08337.

> Absolute quantum yield of the Y-CDs and the TEM image of Y-CDs, the size distributions of the Y-CDs (PDF)

■ AUTHOR INFORMATION

Corresponding Author

Yan Wu − *College of Furnishings and Industrial Design, Nanjing Forestry University, Nanjing 210037, China; Co-Innovation Center of Efficient Processing and Utilization of Forest Resources, Nanjing Forestry University, Nanjing 210037, China*; Email: wuyan@njfu.edu.cn

Authors

Rui Xu − *College of Furnishings and Industrial Design, Nanjing Forestry University, Nanjing 210037, China; Co-Innovation Center of Efficient Processing and Utilization of Forest Resources, Nanjing Forestry University, Nanjing 210037, China;* ⓘ orcid.org/0009-0005-6180-8489

Jian Gan − *Co-Innovation Center of Efficient Processing and Utilization of Forest Resources, Nanjing Forestry University, Nanjing 210037, China*

Jing Wang − *College of Engineering and Applied Sciences, Nanjing University, Nanjing 210023, China*

Weiying Zhao − *College of Furnishings and Industrial Design, Nanjing Forestry University, Nanjing 210037, China; Co-Innovation Center of Efficient Processing and Utilization of Forest Resources, Nanjing Forestry University, Nanjing 210037, China;* orcid.org/0009-0008-4941-0939

Ke Tong − *College of Furnishings and Industrial Design, Nanjing Forestry University, Nanjing 210037, China; Co-Innovation Center of Efficient Processing and Utilization of Forest Resources, Nanjing Forestry University, Nanjing 210037, China*

Complete contact information is available at:
https://pubs.acs.org/10.1021/acsomega.3c08337

■ REFERENCES

(1) Zhao, D.; et al. The influence of solar ultraviolet radiation on human body. *China Sci. Technol. Inf.* **2018**, *Z1*, 43−44.

(2) Andrady, A.; Hamid, H.; Torikai, A. Effects of solar UV and climate change on materials. *Photochem. Photobiol. Sci.* **2011**, *10* (2), 292−300.

(3) Zhou, Y.; Fan, F.; Liu, Y.; Zhao, S.; Xu, Q.; Wang, S.; Luo, D.; Long, Y. Unconventional smart windows: Materials, structures and designs. *Nano Energy* **2021**, *90*, 106613.

(4) Wu, Y.; Zhou, J.; Huang, Q.; Yang, F.; Wang, Y.; Wang, J. Study on the Properties of Partially Transparent Wood under Different Delignification Processes. *Polymers* **2020**, *12* (3), 661.

(5) Mi, R.; Li, T.; Dalgo, D.; Chen, C.; Kuang, Y.; He, S.; Zhao, X.; Xie, W.; Gan, W.; Zhu, J.; Srebric, J.; Yang, R.; Hu, L. A Clear, Strong, and Thermally Insulated Transparent Wood for Energy Efficient Windows. *Adv. Funct. Mater.* **2020**, *30* (23), 2001291.

(6) Gan, W.; Xiao, S.; Gao, L.; Gao, R.; Li, J.; Zhan, X. Luminescent and transparent wood composites fabricated by poly (methyl methacrylate) and gamma-Fe2O3@YVO4:Eu3+ nanoparticle impregnation. *ACS Sustain. Chem. Eng.* **2017**, *5* (5), 3855−3862.

(7) Mi, R.; Chen, C.; Keplinger, T.; Pei, Y.; He, S.; Liu, D.; Li, J.; Dai, J.; Hitz, E.; Yang, B.; et al. Scalable aesthetic transparent wood for energy efficient buildings. *Nat. Commun.* **2020**, *11*, 3836.

(8) Wang, Y.; Wu, Y.; Yang, F.; Yang, L.; Wang, J.; Zhou, J.; Wang, J. A highly transparent compressed wood prepared by cell wall densification. *Wood Sci. Technol.* **2022**, *56* (2), 669−686.

(9) Li, H.; Guo, X.; He, Y.; Zheng, R. A green steam-modified delignification method to prepare low-lignin delignified wood for thick, large highly transparent wood composites. *J. Mater. Res.* **2019**, *34* (6), 932−940.

(10) Fu, Q.; Yan, M.; Jungstedt, E.; Yang, X.; Li, Y.; Berglund, L. A. Transparent plywood as a load-bearing and luminescentbiocomposite. *Compos. Sci. Technol.* **2018**, *164*, 296−303.

(11) Li, Y.; Yu, S.; Veinot, J. G. C.; Linnros, J.; Berglund, L.; Sychugov, I. Luminescent Transparent Wood. *Adv. Opt. Mater.* **2017**, *5*, 1600834.

(12) Gan, W.; Gao, L.; Xiao, S.; Zhang, W.; Zhan, X.; Li, J. Transparent magnetic wood composites based on immobilizingFe₃O₄

nanoparticles into a delignified wood template. *J. Mater. Sci.* **2017**, *52* (6), 3321−3329.

(13) Gan, W.; Gao, L.; Xiao, S.; Zhang, W.; Zhan, X.; Li, J. Transparent Magnetic Wood Composites Based on Immobilizing Fe3O4 Nanoparticles into a Delignified Wood Template. *J. Mater. Sci.* **2017**, *52*, 3321−3329.

(14) Montanari, C.; Ogawa, Y.; Olsén, P.; Berglund, L. A. High performance, fully bio-based, and optically transparent wood biocomposites. *Adv. Sci.* **2021**, *8* (12), 2100559.

(15) Yu, Z.; Yao, Y.; Yao, J.; Zhang, L.; Chen, Z.; Gao, Y.; Luo, H. Transparent Wood Containing Csxwo3 Nanoparticles for Heat-Shielding Window Applications. *J. Mater. Chem. A* **2017**, *5* (13), 6019−6024.

(16) Wang, J.; Wu, X.; Wang, Y.; Zhao, W.; Zhao, Y.; Zhou, M.; Wu, Y.; Ji, G. Green, Sustainable Architectural Bamboo with High Light Transmission and Excellent Electromagnetic Shielding as a Candidate for Energy-Saving Buildings. *Nano-Micro Lett.* **2023**, *15*, 11.

(17) Qiu, Z.; Xiao, Z.; Gao, L.; Li, J.; Wang, H.; Wang, Y.; Xie, Y. Transparent wood bearing a shielding effect to infrared heat andultraviolet via incorporation of modified antimony-doped tin oxide nanoparticles. *Compos. Sci. Technol.* **2019**, *172*, 43−48.

(18) Kang, H.; Guo, Y.; Li, J. Research progress of ultraviolet shielding nanomaterials and their improvement of wood photoaging resistance. *Wood Sci. Technol.* **2002**, *36* (03), 1−9.

(19) Wang, L.; Li, W. T.; Yin, L. Q.; Liu, Y. J.; Guo, H. Z.; Lai, J. W.; Han, Y.; Li, G.; Li, M.; Zhang, J.; Vajtai, R.; Ajayan, P.; Wu, M. Full-color fluorescent carbon quantum dots. *Sci. Adv.* **2020**, *6* (40), 6772.

(20) Ren, J.; Stagi, L.; Innocenzi, P. Fluorescent carbon dots in solidstate: From nanostructures to functional devices. *Prog. Solid State Chem.* **2021**, *62*, 100295.

(21) Zhao, H.; Benetti, D.; Tong, X.; Zhang, H.; Zhou, Y.; Liu, G.; Ma, D.; Sun, S.; Wang, Z.; Wang, Y.; Rosei, F. Efficient and stable tandem luminescent solar concentrators based on carbon dots and perovskite quantum dots. *Nano Energy* **2018**, *50*, 756−765.

(22) Zhao, H.; Liu, G.; You, S.; Camargo, F.; Zavelani-Rossi, M.; Wang, X.; Sun, C.; Liu, B.; Zhang, Y.; Han, G.; et al. Gram-scale synthesis of carbon quantum dots with a large Stokes shift for the fabrication of eco-friendly and high-efficiency luminescent solar concentrators. *Energy Environ. Sci.* **2021**, *14* (1), 396−406.

(23) Gan, J.; Chen, L.; Chen, Z.; Zhang, J.; Yu, W.; Huang, C.; Wu, Y.; Zhang, K. Lignocellulosic Biomass-Based Carbon Dots: Synthesis Processes, Properties, and Applications. *Small* **2023**, *19*, 2304066.

(24) Qu, S.; Wang, X.; Lu, Q.; Liu, X.; Wang, L. A biocompatible fluorescent ink based on water-soluble luminescent carbon nanodots. *Angew. Chem.* **2012**, *124* (49), 12381−12384.

(25) Gan, J.; Wu, Y.; Yang, F.; Wu, X.; Wang, Y.; Wang, J. UV-Filtering Cellulose Nanocrystal/Carbon Quantum Dot Composite Films for Light Conversion in Glass Windows. *ACS Appl. Nano Mater.* **2021**, *4*, 12552−12560.

(26) Mosconi, D.; Mazzier, D.; Silvestrini, S.; Privitera, A.; Marega, C.; Franco, L.; Moretto, A. Synthesis and Photochemical Applications of Processable Polymers Enclosing Photoluminescent Carbon Quantum Dots. *ACS Nano* **2015**, *9*, 4156−4164.

(27) Wu, Y.; Wang, Y.; Yang, F. Comparison of Multilayer Transparent Wood and Single Layer Transparent Wood With the Same Thickness. *Front. Mater.* **2021**, *8*, 63345.

(28) Wang, X.; Zhang, Y.; Luo, J.; Xu, T.; Si, C.; Oscanoa, A.; Tang, D.; Zhu, L.; Wang, P.; Huang, C. Printability of hybridized composite from maleic acid-treated bacterial cellulose with gelatin for bone tissue regeneration. *Adv. Compos. Hybrid Mater.* **2023**, *6*, 134.

(29) Pei, W.; Yusufu, Y.; Zhan, Y.; Wang, X.; Gan, J.; Zheng, L.; Wang, P.; Zhang, K.; Huang, C. Biosynthesizing lignin dehydrogenation polymer to fabricate hybrid hydrogel composite with hyaluronic acid for cartilage repair. *Adv. Compos. Hybrid Mater.* **2023**, *6*, 180.

(30) Wang, Y.; Wu, Y.; Yang, F.; Wang, J.; Zhou, J. A multilayer transparent wood prepared by laminating two kinds of tree species. *J. Appl. Polym. Sci.* **2021**, *139*, No. e51872.

(31) Sun, S. C.; Sun, S. F.; Xu, Y.; Wen, J. L.; Yuan, T. Q. Green and sustainable production of high-purity lignin microparticles with well-

preserved substructure and enhanced anti-UV/oxidant activity using peroxide-promoted alkaline deep eutectic solvent. *Int. J. Biol. Macromol.* **2023**, *253*, 127057.

(32) Wang, Z.; Yuan, F.; Li, X.; Li, Y.; Zhong, H.; Fan, L.; Yang, S. 53% Efficient Red Emissive Carbon Quantum Dots for High Color Rendering and Stable Warm White-Light-Emitting Diodes. *Adv. Mater.* **2017**, *29* (37), 1702910.

(33) Ye, Q.; Yan, F.; Luo, Y.; Wang, Y.; Zhou, X.; Chen, L. Formation of N, S-codoped fluorescent carbon dots from biomass and their application for the selective detection of mercury and iron ion. *Spectrochim. Acta, Part A* **2017**, *173*, 854−862.

(34) Yin, C.; Chen, L.; Niu, N. Nitrogen-doped carbon quantum dots fabricated from cellulolytic enzyme lignin and its application to the determination of cytochrome c and trypsin. *Anal. Bioanal. Chem.* **2021**, *413*, 5239−5249.

(35) Zhang, B.; Liu, Y.; Ren, M.; Li, W.; Zhang, X.; Vajtai, R.; Ajayan, P. M.; Tour, J. M.; Wang, L. Sustainable Synthesis of Bright Green Fluorescent Nitrogen-Doped Carbon Quantum Dots from Alkali Lignin. *ChemSusChem* **2019**, *12*, 4202−4210.

(36) Li, Q.; Zhou, M.; Yang, Q.; Wu, Q.; Shi, J.; Gong, A.; Yang, M. Efficient Room-Temperature Phosphorescence from Nitrogen-Doped Carbon Dots in Composite Matrices. *Chem. Mater.* **2016**, *28*, 8221−8227.

(37) Tan, J.; Zou, R.; Zhang, J.; Li, W.; Zhang, L.; Yue, D. Large-scale synthesis of N-doped carbon quantum dots and their phosphorescence properties in a polyurethane matrix. *Nanoscale* **2016**, *8*, 4742−4747.

(38) Jiang, K.; Wang, Y.; Cai, C.; Lin, H. Conversion of Carbon Dots from Fluorescence to Ultralong Room-Temperature Phosphorescence by Heating for Security Applications. *Adv. Mater.* **2018**, *30*, 1800783.

(39) Jiang, K.; Wang, Y.; Gao, X.; Cai, C.; Lin, H. Facile, Quick, and Gram-Scale Synthesis of Ultralong-Lifetime Room-Temperature-Phosphorescent Carbon Dots by Microwave Irradiation. *Angew. Chem., Int. Ed.* **2018**, *57*, 6216−6220.

(40) Liu, Y.; Yang, H.; Ma, C.; Luo, S.; Xu, M.; Wu, Z.; Li, W.; Liu, S. Luminescent Transparent Wood Based on Lignin-Derived Carbon Dots as a Building Material for Dual-Channel, Real-Time, and Visual Detection of Formaldehyde Gas. *ACS Appl. Mater. Interfaces* **2020**, *12*, 36628−36638.

(41) Zhang, C.; Lin, T.; Yin, X.; et al. Preparation of transparent wood containing carbon dots for application in the Field of white-LED. *J. Wood Chem. Technol.* **2022**, *42*, 331−341.

(42) Zhang, Y.; Yu, Y.; Lu, Y.; Yu, W.; Wang, S. Effects of heat treatment on surface physicochemical properties and sorption behavior of bamboo (phyllostachys edulis). *Constr. Build. Mater.* **2021**, *282*, 122683.

(43) Zhao, Z.; Zhang, X.; Lin, Q.; Zhu, N.; Gui, C.; et al. Development and investigation of a two-component adhesive composed of soybean four and sugar solution for plywood manufacturing. *Wood Mater. Sci. Eng.* **2023**, *18*, 884−892.

(44) Gan, J.; Wu, Y.; Yang, F.; Zhang, H.; Wu, X.; Wang, Y.; Xu, R. Wood-cellulose photoluminescence material based on carbon quantum dot for light conversion. *Carbohydr. Polym.* **2022**, *290*, 119429.

(45) Zhang, H.; Gan, J.; Wu, Y.; Wu, Z. Biomimetic high water adhesion superhydrophobic surface via UV nanoimprint lithography. *Appl. Surf. Sci.* **2023**, *633*, 157610.